CHAPTER

Singularity analysis in quantum chemistry

9

David Z. Goodson

Department of Chemistry and Biochemistry, University of Massachusetts Dartmouth, North Dartmouth, MA, United States

1 MATHEMATICAL BACKGROUND

Complex analysis is a branch of mathematics with widespread applications in mathematical physics [1,2]. One of its core strategies is to develop approximate descriptions of unknown functions by allowing the variable to range over the complex numbers, and then analyzing the behavior in the neighborhoods of special points in the complex plane, called *singularities*, where the functions become poorly defined. This chapter describes various applications of singularity analysis to the Schrödinger equation. The function in question is the energy of an atom or molecule and the variable is some parameter that affects the energy, such as a bond distance, or a nuclear charge, or an artificial parameter in a perturbation theory.

Let us begin with a simple example. The Schrödinger equation is typically solved within a finite basis-set approximation, with the wavefunction Ψ expressed as a linear combination

$$\Psi = \sum_{j=1}^{N} a_j \psi_j, \tag{1}$$

in terms of a set of N linearly independent functions ψ_j. This is conveniently formulated as a matrix eigenvalue equation,

$$\mathbf{H}\boldsymbol{a} = E\boldsymbol{a}, \tag{2}$$

where $\boldsymbol{a}$ is an N-dimensional column vector of the unknown coefficients a_j and $\mathbf{H}$ is an $N \times N$ matrix of the scalar values $H_{jk} = \langle \psi_j | H | \psi_k \rangle$ constructed from the Hamiltonian operator H for each of the N possible values of j and k. N, the size of the basis set, is referred to as the basis set's *dimension*. The eigenvalues E approach

Mathematical Physics in Theoretical Chemistry. https://doi.org/10.1016/B978-0-12-813651-5.00009-7

the true eigenvalues as N approaches infinity. We are interested here in how the eigenvalues depend on some parameter λ that appears explicitly in the Hamiltonian.

Eq. (2) is usually solved with some numerical approximation method, but it is informative to consider a simple case that can be solved analytically. Consider a Hamiltonian that can be written in the form

$$H(\lambda) = h + \lambda v, \tag{3}$$

where the operators h and v are independent of λ, with a basis of dimension $N = 2$. Let us consider in particular the case with, for $j \neq k$, matrix elements $h_{jk} = 0$ and $v_{jk} = v_{kj} = w$,

$$\left[\begin{pmatrix} h_{11} & 0 \\ 0 & h_{22} \end{pmatrix} + \lambda \begin{pmatrix} v_{11} & w \\ w & v_{22} \end{pmatrix}\right] \begin{pmatrix} a_1 \\ a_2 \end{pmatrix} = E \begin{pmatrix} a_1 \\ a_2 \end{pmatrix}. \tag{4}$$

This is a system of two simultaneous linear equations in the coefficients a_1 and a_2 that can be solved to give two solutions for the energy E as a function of λ,

$$E(\lambda) = \frac{h_{11} + h_{22}}{2} + \lambda \frac{v_{11} + v_{22}}{2} \pm \frac{1}{2} \left(\delta_v^2 + 4w^2\right)^{1/2} \sqrt{(\lambda_s - \lambda)(\lambda_s^* - \lambda)}, \tag{5}$$

where $\delta_v = v_{11} - v_{22}$ and

$$\lambda_s = \frac{h_{22} - h_{11}}{\delta_v^2 + 4w^2}(\delta_v + 2wi), \quad \lambda_s^* = \frac{h_{22} - h_{11}}{\delta_v^2 + 4w^2}(\delta_v - 2wi), \tag{6}$$

with $i = \sqrt{-1}$. One can see from Eq. (4) that the parameter w is responsible for the coupling between the equations for a_1 and a_2.

Fig. 1 shows the distinctive behavior of the two solutions for $E(\lambda)$. The left panel shows $E(\lambda)$ for values of λ along the real axis of the complex λ-plane. There is an avoided crossing with the closest approach occurring at the value of λ equal to $\mathrm{Re}\,\lambda_s$. The spacing between the curves at closest approach is

$$\Delta E_{\min} = \frac{2|(h_{22} - h_{11})w|}{\sqrt{\delta_v^2 + 4w^2}}. \tag{7}$$

This decreases with decreasing w. For very small w the curves would come so close that they would appear, under low resolution, to pass through each other. Physical properties correspond to *real* numbers. Nevertheless, this example demonstrates that the existence of singular points at nonphysical parameter values, in the complex plane, can affect the behavior of the real, physical, solution.

The right panel of Fig. 1 shows the real parts of the two solutions for $E(\lambda)$ along a diagonal path through the complex plane passing through the origin and the singular point in the upper half-plane. Note the kinks, at $\lambda = \lambda_s$, where the two eigenvalues become equal. The slopes at that point become infinite. The general definition of a *singular point* (or *singularity*, for short) is a point at which the function and/or its first derivative becomes infinite or undefined.

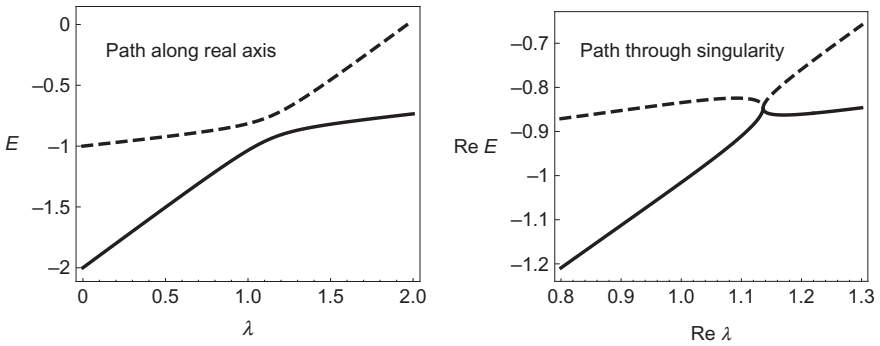

FIG. 1

Eigenvalues of Eq. (4), a 2×2 matrix eigenvalue equation with parameters $h_{11} = -2$, $h_{22} = -1$, $v_{11} = 1$, $v_{22} = 0.15$, and $w = 0.08$, which lead to branch points at $1.136 \pm 0.214i$. The eigenvalues are shown along two paths in the complex λ-plane; the *left panel* corresponds to a path along the real axis while the *right panel* corresponds to a path along the straight line that passes through $\lambda = 0$ and $\lambda = 1.136 + 0.214i$. The *solid curves* show the lower eigenvalue while the *dashed curves* show the upper eigenvalue.

The singularities of the matrix eigenvalue problem are an example of an important class of singularities called *branch points*. If one follows one of the two $E(\lambda)$ functions along a path in the complex λ-plane that completely encircles λ_s, then it will switch to the other function. Thus the two eigenvalue solutions, one with the "$-$" sign and the other with the "$+$" sign, can be thought of as two branches of a single function in the complex plane. To see how this happens in Eq. (5), consider a circular path of radius β centered at λ_s. This can be described in terms of an angle θ according to

$$\lambda = \lambda_s - \beta(\cos\theta + i\sin\theta) = \lambda_s - \beta e^{i\theta}. \tag{8}$$

(The second equality follows from Euler's relation, the definition of the exponential of a complex number [1].) As θ goes from 0 to 2π, the factor

$$(\lambda_s - \lambda)^{1/2} = \beta^{1/2} e^{i\theta/2} \tag{9}$$

in Eq. (5) goes from $\beta^{1/2}$ to $\beta^{1/2} e^{i\pi} = -\beta^{1/2}$, switching the square root's sign.

In this particular case, we have a *square-root* branch point; the singular behavior results from the square root in Eq. (5). The main focus of this chapter will be square-root branch points. The matrix eigenvalue equation for arbitrary finite dimension N was analyzed by Katz [3] in the context of nuclear physics. The exact analytical solution is not in general available at higher dimension, but Katz was able to prove that for nondegenerate eigenvalues $E_0(\lambda)$, $E_1(\lambda)$, $E_2(\lambda)$, ..., $E_N(\lambda)$ for states of the same symmetry (i.e., the same values of angular momentum quantum numbers), there

exists in general a complex-conjugate pair of square-root branch points λ_{jk} and λ_{jk}^* with nonzero imaginary parts that connect the eigenvalues $E_j(\lambda)$ and $E_k(\lambda)$ for any combination of j and k.

Branch points are not the only kind of singularity. For example, a function

$$f(\lambda) = \frac{c}{(\lambda_s - \lambda)^m}, \tag{10}$$

where m is a positive integer and c is a constant, is said to have a *pole* of order m at $\lambda = \lambda_s$. The function and its derivative are infinite at λ_s but there is only one branch.

Another kind of singularity is a *critical point*, a point at which the qualitative nature of the solution undergoes a sudden transition. These occur, for example, in thermodynamics when the system undergoes a phase transition. The singularities corresponding to phase transitions are branch points. Their explicit functional forms are usually unknown, but they are much more complicated than simple algebraic branch points. In contrast to the branch points of the matrix eigenvalue problem, the critical point lies *on* the real axis.

2 AVOIDED CROSSINGS OF MOLECULAR POTENTIAL ENERGY

2.1 BORN-OPPENHEIMER APPROXIMATION

The Schrödinger equation for a diatomic molecule can be formulated as a matrix eigenvalue equation as in Eq. (2), with λ corresponding to the distance x between the two atomic nuclei. Let N_e be the number of electrons. We will assume that the kinetic energy operator, in atomic units, can be expressed as

$$T = -\frac{1}{2}\sum_{j=1}^{N_e} \nabla_j^2, \tag{11}$$

where N_e is the number of electrons. This follows from the Born-Oppenheimer approximation, according to which the kinetic energy operators for nuclear motions are omitted because the nuclear masses are each much larger than the mass of an electron. The potential energy from electron-electron repulsion is

$$W = \sum_{j=1}^{N_e-1} \sum_{k=j+1}^{N_e} r_{jk}^{-1}, \tag{12}$$

where r_{jk} is the distance between electron j and electron k. The potential energy for nucleus-electron attraction for a diatomic molecule is

$$U(x) = -\sum_{j=1}^{N_e} \left(\frac{Z_1}{\rho_{1j}} + \frac{Z_2}{\rho_{2j}} \right), \tag{13}$$

where ρ_{1j} and ρ_{2j} are, respectively, the distance between electron j and nucleus 1 and the distance between electron j and nucleus 2. Z_1 and Z_2 are the atomic numbers of the nuclei (i.e., the nuclear charges in atomic units). The Hamiltonian, then, is

$$H(x) = T + U(x) + W, \tag{14}$$

and the dependence on x comes only from the expressions for $\rho_{1,j}$ and $\rho_{2,j}$, which depend on the relative positions of the nuclei.

We can write an electronic Schrödinger equation as

$$H(x)\Psi = \epsilon(x)\Psi. \tag{15}$$

The total energy of the molecule is obtained by adding to the electronic energy $\epsilon(x)$ the potential energy of internuclear repulsion,

$$E(x) = \epsilon(x) + Z_1 Z_2/x. \tag{16}$$

$E(x)$ can be treated as the potential energy for the dynamics of the nuclei.

Expressing Ψ in terms of some appropriate set of basis functions ψ_j according to Eq. (1) leads to a matrix eigenvalue equation for $\epsilon(x)$. If the basis set is constructed from Hartree-Fock atomic orbitals, then this is called the *full configuration interaction* (FCI) solution. This method reliably converges to the solution for ϵ with increasing basis-set size N, and what we obtain is a set of numerical values for $\epsilon(x)$ at an arbitrary selection of discrete values for internuclear separation x. The left panel of Fig. 2 shows benchmark FCI results for the hydrogen fluoride molecule for the

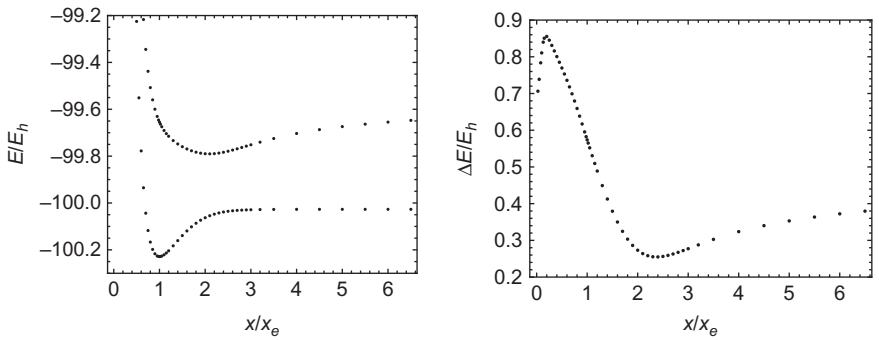

FIG. 2

Potential energy values for the hydrogen fluoride molecule, for the ground state and the first excited state of the same symmetry, from numerical solution of the matrix eigenvalue problem. (These results are from full configuration-interaction calculations within the cc-pVDZ basis set. See Ref. [4] for details.) The *left panel* shows the functions $E(x)$ and the *right panel* shows the difference between them. The internuclear distance is in units of the equilibrium bond length, $x_e = 0.92025$ Å and energy is in units of hartrees.

ground-state energy and for the first excited state of the same symmetry as the ground state, for discrete values of x over a wide range. The right panel of the figure shows the difference between the two eigenvalues. The closest approach is seen to occur at x/x_e between 2.3 and 2.4. It is only for the 2×2 matrix eigenvalues that closest approach will occur exactly at the real part of a branch point. However, we can expect that the real part of the branch point in this case will be somewhere in this vicinity.

2.2 INTERPOLATION WITH QUADRATIC APPROXIMANTS

Our goal now is use our knowledge of the nature of the singularity structure to construct from a discrete set of energy values a continuous analytical function that interpolates between them. Consider an arbitrary function $f(x)$ and suppose we have a dataset of K discrete points,

$$\{(x_1,f_1),(x_2,f_2),(x_3,f_3),\ldots,(x_K,f_K)\},$$

with $f_j = f(x_j)$. Let us define three polynomials,

$$P(x) = p_0 + p_1 x + p_2 x^2 + \cdots + p_{M_p} x^{M_p}, \tag{17}$$

$$Q(x) = 1 + q_1 x + q_2 x^2 + \cdots + q_{M_q} x^{M_q}, \tag{18}$$

$$R(x) = r_0 + r_1 x + r_2 x^2 + \cdots + r_{M_r} x^{M_r}, \tag{19}$$

such that

$$Q(x_j) f_j^2 - P(x_j) f_j + R(x_j) = 0 \tag{20}$$

for each point in the dataset. Dividing both sides of Eq. (20) by a constant has no effect on the solution. Therefore, one of the polynomial coefficients is arbitrary. It is traditional to account for this by setting $q_0 = 1$.

Eq. (20) is a set of K simultaneous equations that determine the values of the polynomial coefficients p_j, q_j, and r_j. We have $M_p + M_q + M_r + 2$ coefficients and K equations. Therefore, we must choose values M_p, M_q, M_r such that

$$M_p + M_q + M_r = K - 2. \tag{21}$$

If we solve Eq. (20) for arbitrary x_j we obtain

$$f_j = \frac{1}{2Q(x_j)} \left[P(x_j) \pm \sqrt{P(x_j)^2 - 4Q(x_j)R(x_j)} \right]. \tag{22}$$

This suggests that we model the function with

$$S(x) = \frac{1}{2Q(x)} \left[P(x) \pm \sqrt{P(x)^2 - 4Q(x)R(x)} \right]. \tag{23}$$

$S(x)$ is called a *quadratic approximant*.[1] It interpolates between the points in the dataset, because by construction $S(x_j) = f_j$, and, very importantly, it can model square-root branch points. $S(x)$ will generally have square-root branch points at x values in the complex plane that are roots of the discriminant polynomial; that is, x values for which

$$P(x)^2 - 4Q(x)R(x) = 0. \tag{24}$$

Quadratic approximants are a convenient tool for modeling functions that contain branch points. However, to take full advantage of their capabilities requires some thought. It is a good idea to incorporate into the approximant whatever we know in advance about the functional form of $\epsilon(x)$. Consider its behavior in the limit $x \to \infty$. This is the limit of dissociation into molecular fragments. For the hydrogen fluoride molecule this would be neutral isolated H and F atoms. Therefore, we want each branch of $S(x)$ to approach a different finite negative value. (Negative because the fragments are in bound electronic states.) For very large x we have

$$S(x) \sim \frac{1}{2q_{M_q}x^{M_q}}\left[p_{M_p}x^{M_p} \pm \left(p_{M_p}^2 x^{2M_p} - 4q_{M_q}r_{M_r}x^{M_q+M_r}\right)^{1/2}\right], \tag{25}$$

which will have the desired behavior only if both of the terms in the square brackets are proportional to x^{M_q} in the large-x limit. It follows that the only reasonable choice for the degrees of the three polynomials for this application is

$$M_p = M_q = M_r \equiv M. \tag{26}$$

Suppose that the sum of the energies of the dissociated fragments in the ground state is a known value $E_{\mathrm{d},0}$, and in an excited state is a known value $E_{\mathrm{d},1}$. (If we can calculate molecular energies, then it should be even easier to calculate the energies of the fragments, because each fragment has fewer electrons than does the original molecule.) Setting Eq. (25) equal to these values gives

$$p_M = (E_{\mathrm{d},0} + E_{\mathrm{d},1})q_M, \quad r_M = E_{\mathrm{d},0}E_{\mathrm{d},1}q_M. \tag{27}$$

A possible source of difficulty comes from the fact that $S(x)$ can have more branch points than needed. For the true $E(x)$, the branch point pair connecting the ground state with the excited state shown in Fig. 2, with real part $2.36\,x_{\mathrm{e}}$, is the only one that strongly affects the behavior of the ground state in the regions of the potential that are of practical interest. There is a weak avoided crossing of the ground state with the next higher excited state at a much larger bond distance. There is also a complicated collection of closely spaced avoided crossings at internuclear distances less than $0.3\,x_{\mathrm{e}}$, but because the potential energy is so high for such small internuclear

[1] Quadratic approximants were proposed in the 19th century but attracted little attention until they were rediscovered in the 1970s. Since then, a variety of applications has been found for them in different areas of physics. The idea of using them for molecular potential energies comes from Jordan [5].

distances, this region will not usually be of importance for chemical dynamics and will usually not be well enough represented in the dataset for the approximants to accurately model the corresponding branch points. Thus, at least in this case, we really only have one branch point pair concerning which the dataset provides much information. However, the number of branch points in the diagonal approximant is equal to the number of roots of the polynomial $P^2 - QR$. This is $2M$, which can be much larger than needed.

The approximants dispose of superfluous branch points in a few different ways. One way is to place them at distant points in the complex plane, far from the region of the real axis being modeled. These cause no problem. Another way is to have pairs of nearly coincident branch points. Suppose a point x_s is a double root. Then the square-root term in the approximant will be proportional to $\sqrt{(x - x_s)^2} = x - x_s$, which is in fact *not* singular. In practice the roots are not exactly coincident, which means that in their immediate vicinity $S(x)$ will have spurious singular behavior. If they are located near the real axis in the physically interesting region, this can be problematic. However, their positions typically shift with increasing M, which distinguishes them from physical branch points.

There is another kind of spurious singularity. Consider a point x_s on the positive real axis at which the denominator polynomial goes to zero; that is, $Q(x_s) = 0$. The lower branch of the approximant (with the minus sign) is not obviously affected. As x approaches x_s, $S(x)$ smoothly approaches $R(x_s)/P(x_s)$ with no singular behavior. However, for the upper branch (with the plus sign) in the neighborhood of x_s we have

$$S(x) \sim \frac{P(x)}{Q(x)} \sim \frac{c}{x_s - x}, \quad x \to x_s, \tag{28}$$

where c is a constant, which is a first-order pole. This singularity is completely spurious but it has a huge effect on the upper branch.

An easy way to prevent a pole on the positive real axis is to use

$$Q(x) = 1 + q_M x^M \tag{29}$$

as the denominator polynomial and then treat q_M as an arbitrary parameter. If q_M is chosen to be a positive real number, then $Q(x)$ will have no zeros on the positive real axis. Furthermore, one can take advantage of q_M as a free parameter by choosing it so as to optimize the approximant's branch point structure, moving spurious branch points away from the region of interest. The positions of spurious branch points will shift with changing q_M while physical branch points will remain stable.

We have $2M$ parameters still to be determined: $p_0, p_1, p_2, \ldots, p_{M-1}$ and $r_0, r_1, r_2, \ldots, r_{M-1}$. For a given M value we will need a dataset of $K = 2M$ points on the potential energy curve. The parameters are obtained from K simultaneous algebraic equations given by Eq. (20). The approximant $S(x)$ will give an interpolation between these points and, with its second branch, a prediction for the excited state.

Suppose that at some or all of the x_j the dataset includes the energy of the excited state as well as that of the ground state. It is easy to include this in the parameterization. If we add together the two branches of $S(x)$, given by Eq. (23), we get an approximant for the sum of the energies. It follows that

$$P(x_j) - (E_{j,0} + E_{j,1})Q(x_j) = 0. \tag{30}$$

These are additional linear equations, which we solve along with those for the ground-state energy from Eq. (20).

Fig. 3 shows that the quadratic approximants can give an accurate analytical expression for modeling the potential energy over a wide range of x. The upper panel shows a result from parameterization to a dataset including only ground-state energies. The dashed curves show the upper branch of the approximant for two different choices of q_M. The lower branch is virtually unchanged over a wide range of q_M, but the upper branch is strongly affected. However, the location of the dominant branch point is quite stable. Both cases in the figure have branch points at $2.0 \pm 0.9i$. The fact that the upper curve poorly models the excited state is due to the fact that $S(x)$ has only two branches, while the solution to the $N \times N$ matrix formulation of the Schrödinger equation has N branches. The upper branch of $S(x)$ models different excited states in different regions of x. In particular, at small x, where avoided crossings occur between the ground state and higher excited states, the upper branch will switch to a higher eigenstate. A relatively smaller value of q_M has the effect of giving greater weight to data points at smaller x. The lower panel of Fig. 3 demonstrates that the upper branch can be constrained to the first excited state by including some excited-state energies in the dataset.

The ability of quadratic approximants to describe the behavior in the vicinity of an avoided crossing nicely complements various computationally efficient but less accurate methods for solving the Schrödinger equation. For molecules with more than 10 or so electrons, the matrix eigenvalue problem with an appropriately large basis set becomes computationally intractable. More efficient computational methods, however, involve further approximations and these approximations can be particularly inaccurate near an avoided crossing.

The approximations typically are based on the assumption that the true wavefunction is described reasonably well by a single Hartree-Fock orbital configuration. This assumption fails as the bond is stretched into the avoided crossing region, where the wavefunction is more accurately described by a linear combination of two different orbitals, corresponding to the interacting eigenstates. Another problem arises from the treatment of spin. "Unrestricted" methods are based on an approximate wavefunction that is not an eigenfunction of the spin operator. In practice this fact does not significantly affect the accuracy of the energy if x is close to the equilibrium bond distance or if x is very large, approaching dissociation. However, at intermediate bond distances the approximate wavefunction will be a linear combination of orbitals with different spin eigenvalues and this will adversely affect the accuracy. It is possible to formulate approximate methods so as to restrict the wavefunction to the correct

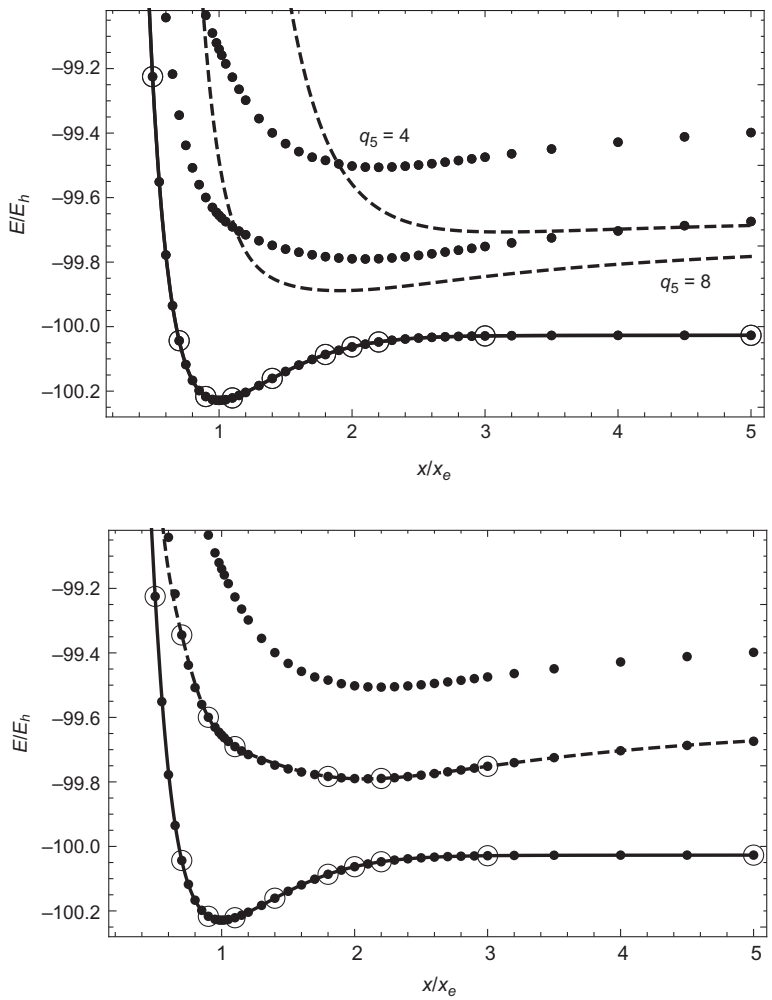

FIG. 3

Quadratic approximants for the potential energy curves of the ground state and the first excited state of the same symmetry for the hydrogen fluoride molecule, using two different datasets. The *dots* show FCI energies for the ground state and the first two excited states of the same symmetry as the ground state. *Circles* mark the points included in the dataset. The *solid curves* show the lower branch of the quadratic approximant while the *dashed curves* show the upper branch. The *upper panel* shows upper branches calculated with two different values of the parameter q_M.

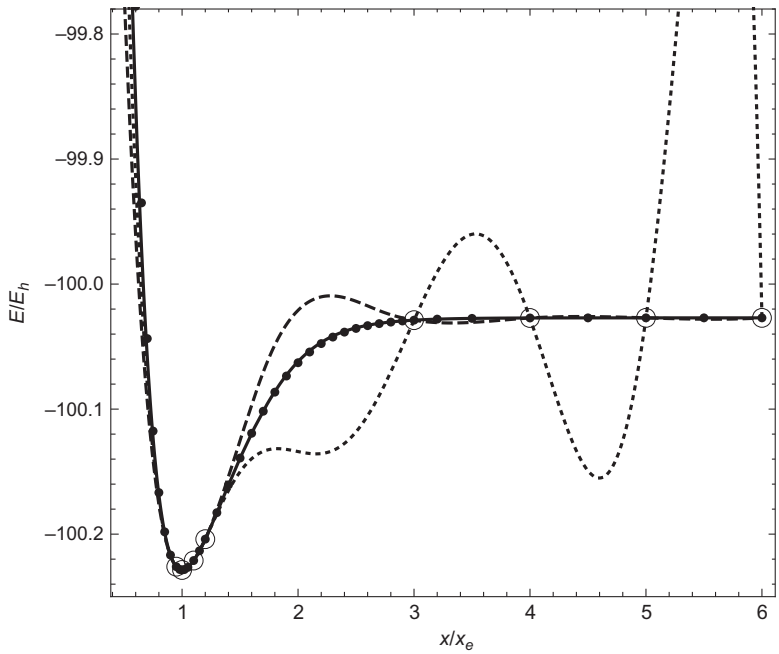

FIG. 4

Comparison of interpolations through the avoided crossing region using a dataset of points outside that region, for the ground-state potential energy curve for hydrogen fluoride. *Dots* indicate correct values. *Circled dots* indicate points used in the dataset for interpolation. The *solid curve* corresponds to the quadratic approximant, $S(x)$. The *dashed curve* shows the cubic spline interpolation while the *dotted curve* shows the interpolation from a seventh-degree polynomial.

spin eigenvalue. Spin restricted formulations of coupled-cluster methods have been found to give better accuracy than the unrestricted version for mildly stretched bonds [6]. Nevertheless, with further stretching restricted methods dissociate incorrectly. For the hydrogen fluoride molecule, for example, restricted methods dissociate into a fluoride anion and a hydrogen cation, rather than the correct limit of two neutral atoms.

Fig. 4 shows the result of interpolation through the avoided crossing region using a dataset that includes only points in the vicinity of the equilibrium bond distance and points at very large internuclear separation. This simulates a situation in which one is using an approximate method that can only give valid results in these two regions. The quadratic approximant predicts the intermediate points virtually exactly within the resolution of this plot. By contrast, the polynomial that interpolates between the eight data points gives a reasonable result only near the equilibrium bond length, and elsewhere it is quite useless. The cubic spline interpolation does fine in the

parameterized regions but in the vicinity of the avoided crossing it is qualitatively incorrect. The polynomial and spline interpolations do not use any information other than the points in the dataset. By contrast, the quadratic approximant, by modeling the expected square-root branch point structure, uses in addition to the dataset, the known mathematical physics of the interaction between the ground state and the first excited state, which influences the shape of the potential energy curve.

3 CRITICAL POINTS IN ELECTRONIC STRUCTURE

3.1 IONIZATION AS A CRITICAL PHENOMENON

The Hamiltonian for an atom with atomic number Z and with N_e electrons can be written

$$H = T + ZU + W, \tag{31}$$

in terms of the kinetic energy operator T (Eq. 11), the potential energy for interelectron repulsion W (Eq. 12), and the potential energy ZU for nucleus-electron attraction, with

$$U = \sum_{j=1}^{N_e} r_j^{-1}, \tag{32}$$

where r_j is the distance between the nucleus and electron j. It is convenient to scale the units of distance by a factor of Z, substituting r_j/Z for r_j, r_{jk}/Z for r_{jk}, and $Z^2\nabla_j^2$ for ∇_j^2. Then the Schrödinger equation can be written

$$H(\lambda)\Psi = E(\lambda)\Psi, \tag{33}$$

where

$$H(\lambda) = T + U + \lambda W \tag{34}$$

and

$$\lambda = 1/Z. \tag{35}$$

The units of energy are now scaled by a factor of Z^2. The unscaled energy can be obtained at the end of the analysis by multiplying E by Z^2. The λ dependence in $H(\lambda)$ is now confined to the interelectron repulsion term λW.

Let us treat λ as a continuous variable. According to Eq. (34), the limit of $\lambda = 0$ represents the turning off of interelectron repulsion, giving a system that is more stable than the physical atom, while increasing λ has the effect of increasing the magnitude of interelectron repulsion. Clearly, there will be some value of λ on the positive real axis beyond which the effect of interelectron repulsion will overwhelm the potential energy of electron-nucleus attraction, and the system will dissociate, releasing an electron. This abrupt change in the character of the system in response to

a continuous change in a parameter is analogous to a phase transition in equilibrium thermodynamics that occurs in response to a continuous change in a state variable, for example, a liquid dissociating into a gas in response to increasing temperature. The parameter value corresponding to the transition is called a *critical* value. Therefore, we will refer to the highest positive real value of λ that can support a fully bound state of the atom as λ_c, the critical λ.

The mathematical manifestation of this phenomenon will be a singularity in $E(\lambda)$ at λ_c, but in contrast to the branch points of the matrix eigenvalue problem, which must have nonzero imaginary parts, the critical point is a singularity *on* the real axis. A sophisticated and laborious analysis [7] of the simplest case, the two-electron atom, showed that $E(\lambda)$ has a branch point at $\lambda_c = 1.09766$ (consistent with the fact that the hydride ion, $\lambda = 1$, is stable in the gas phase) but found that the form of the singularity is more complicated than an algebraic function. The exact functional form of the singularity is not known. When approached from the direction of $\lambda < \lambda_c$ on the real axis, $E(\lambda) - E(\lambda_c)$ approaches 0 in proportion to $(\lambda_c - \lambda)$, but at λ_c the derivative becomes undefined and a path around λ_c causes the function to switch to a different branch.

The Schrödinger equation is usually solved within a basis-set approximation for the wavefunction. This converts Eq. (33) into a matrix eigenvalue equation, which, according to Katz's theorem, can only have square-root branch points, and none of those branch points can lie on the real axis. For an N-dimensional basis set the eigenvalue, will necessarily be nonsingular at λ_c, where we expect the true solution for the energy to be singular.

One might therefore presume that $E_N(\lambda)$ will be useless for studying ionization. In fact, this is not the case. The following section describes a method that uses the expected failure of the matrix formulation as a means to characterize the critical singularity.

3.2 FINITE-SIZE SCALING TO CALCULATE CRITICAL PARAMETERS

In principle, one might determine the value of λ_c by computing $E(\lambda)$ at different λ values and then identifying the critical point as the value of λ at which the energy of the neutral atom becomes equal to that of the $+1$ cation. This is difficult in practice. The true function $E(\lambda)$ is singular at the critical point while the matrix eigenvalue solution for E is nonsingular at that point. At λ values far from λ_c, the influence of the singularity will be small and a relatively small basis set will give high accuracy, but as λ approaches λ_c the size of the basis set will have to be increasingly large to give the same level of accuracy.

While this slowing of the basis-set convergence might be considered a problem, a study of the rate of convergence can be used to advantage to determine the value λ_c indirectly, as the value of λ where the convergence of the energy with increasing basis size begins to significantly slow. This is the rationale of the method of *finite size scaling*, an approach developed in the context of statistical thermodynamics to characterize critical points in thermodynamical state functions [8].

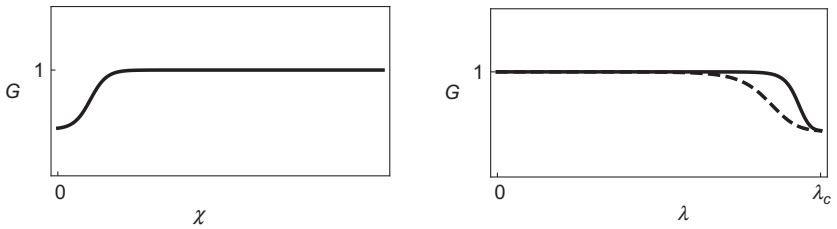

FIG. 5

Expected qualitative behavior of the correction factor $G(\chi)$ of Eq. (36) as a function of χ, and as a function of λ as implied by the scaling postulate, Eq. (37). The *dashed curve* shows the expected behavior for a relatively smaller value of N.

Let us assume that the basis functions do not themselves depend on λ. Then the basic idea is as follows: As the number N of basis functions increases, the neighborhood of λ_c in which the true $E(\lambda)$ is poorly described by the matrix eigenvalue $E_N(\lambda)$ shrinks. Let us introduce a multiplicative correction factor G to describe this situation, such that

$$E - E_c = (E_N - E_c)G, \tag{36}$$

where E_c is the true energy at the critical point, $E(\lambda_c)$. Our expectations for the behavior of G are as follows:

(i) G will be about equal to 1 except in the neighborhood of λ_c.
(ii) The neighborhood in which G significantly deviates from 1 will shrink with increasing N.

The method of finite size scaling is based on a postulate that ensures these expectations are met. Consider G as a function of some variable χ that depends on λ and N such that G rapidly goes to 1 with increasing χ. This is illustrated in the left panel of Fig. 5. As χ approaches 0, G drops below 1, because, according to the variational principle, E_N is an upper bound to E. The finite size scaling postulate is that χ depends on N and λ according to

$$\chi = N(\lambda_c - \lambda)^{\nu}. \tag{37}$$

ν is a parameter whose value we will determine later. $G(\chi)$, using Eq. (37) for χ with ν positive, satisfies our expectations. The first expectation is satisfied because the limit $\lambda \to \lambda_c$ is the same as the limit $\chi \to 0$. The second expectation is satisfied because for given value of λ, increasing N will increase χ, shifting it away from the region of small χ, where G deviates from 1. Thus, N can be thought of as a scale factor for the size of the region in which E_N is inaccurate. This is illustrated in the right panel of Fig. 5. The dashed curve corresponds to a relatively smaller value of N while the solid curve corresponds to a relatively larger value.

The scaling postulate has not been rigorously derived. It is a reasonable guess inspired by qualitative expectations and we will see that it will make it feasible to calculate the value of λ_c without having to solve the much harder problem of calculating G. It was proposed in the 1970s to describe the thermodynamics of magnetization in solids [9]. In that case the parameter N was the number of atomic layers in a thin film. That was a simple example of a more general problem: phase transitions are, strictly speaking, only a property of infinite systems. Thermodynamic functions can be expressed in terms of the partition function, which is an effectively infinite sum over the states of the system. However, if the infinite sum is truncated after a finite number of terms, then it gives a nonsingular function of temperature. This is a close analogy to the basis-set expansion in quantum mechanics. The finite expansion of the partition function can give an accurate description of a bulk system, but the accuracy drops significantly in the neighborhood of the critical temperature, where the system can spontaneously reorganize into a different phase and the true partition function is singular. Finite size scaling has been widely applied in condensed matter physics [8]. The idea of applying it to problems in quantum chemistry comes from Kais et al. [10]. They demonstrated that the scaling postulate gives accurate estimates of λ_c for various model problems in quantum mechanics and then they used the method to estimate critical nuclear charges for atoms and molecules.

In order to computationally study the dependence of E_N on the basis dimension, let us define

$$\Delta_E(\lambda; N_1, N_2) = \ln \frac{E_{N_1}(\lambda) - E_c}{E_{N_2}(\lambda) - E_c} \Big/ \ln \frac{N_2}{N_1} \tag{38}$$

and

$$\Delta'_E(\lambda; N_1, N_2) = \ln \frac{\partial E_{N_1}/\partial\lambda}{\partial E_{N_2}/\partial\lambda} \Big/ \ln \frac{N_2}{N_1}, \tag{39}$$

where N_1 and N_2 are the dimensions for two separate computations of E_N at various different values of λ, using basis functions that are independent of λ. Let us assume that $E(\lambda) - E_c$ is proportional to $(\lambda_c - \lambda)^\alpha$ as λ approaches λ_c from below. (The critical exponent α will be determined later.) In the immediate neighborhood of λ_c it is reasonable to describe E in terms of a series expansion valid as λ approaches λ_c from below, in the form

$$E(\lambda) - E_c \sim (\lambda_c - \lambda)^\alpha \left[\gamma_0 + \gamma_1(\lambda_c - \lambda) + \cdots\right], \quad \lambda_- \to \lambda_c. \tag{40}$$

Let us expand $G(\chi)$ about $\chi = 0$ and then substitute in the scaling postulate for χ. Eq. (36) implies that G will also have to be proportional to $(\lambda_c - \lambda)^\alpha$ in the limit $\lambda_- \to \lambda_c$. It follows that G can be expanded in the form

$$G\left(N(\lambda_c - \lambda)^\nu\right) \sim \left[N(\lambda_c - \lambda)^\nu\right]^{\alpha/\nu} \left[g_0 + g_1 N^{1/\nu}(\lambda_c - \lambda) + \cdots\right], \quad \lambda_- \to \lambda_c. \tag{41}$$

Note that the N and λ dependence appears only in terms of factors of $N(\lambda_c - \lambda)^\nu$. Using the Taylor series $(1+X)^{-1} \sim 1-X$, with $X = (g_1/g_0)N^{1/\nu}(\lambda_c - \lambda)$, we obtain from Eq. (36) the following expansion for E_N about the critical point:

$$E_N(\lambda) - E_c \sim \frac{\gamma_0}{g_0} N^{-\alpha/\nu} \left[1 + \left(\frac{\gamma_1}{\gamma_0} - \frac{g_1}{g_0} N^{1/\nu} \right) (\lambda_c - \lambda) + \cdots \right]. \tag{42}$$

We can now see why Δ_E was defined according to Eq. (38). Its leading-order behavior as λ approaches λ_c is

$$\Delta_E \sim \frac{\ln\left(\frac{N_1}{N_2}\right)^{-\alpha/\nu}}{\ln\left(\frac{N_2}{N_1}\right)} = \frac{\alpha}{\nu}. \tag{43}$$

The important feature to note is that Δ_E becomes independent of N in the limit $\lambda \rightarrow \lambda_c$. If the scaling postulate is valid, then plots of $\Delta_E(\lambda; N_1, N_2)$ versus λ for various different choices of N_1 and N_2 will all intersect when $\lambda = \lambda_c$, at the value α/ν. This is quite useful. It implies that λ_c, the location of the singularity, can be determined using computations of $E_N(\lambda)$, a function that is not singular there.

In order to estimate the value of α, let us define

$$\Gamma_E(\lambda; N_1, N_2) = \frac{\Delta_E}{\Delta_E - \Delta'_E}. \tag{44}$$

It follows from Eq. (42) that

$$\frac{\partial E_N}{\partial \lambda} \sim \frac{\gamma_0 g_1}{g_0^2} N^{(1-\alpha)/\nu} \left(1 - \frac{g_0 \gamma_1}{\gamma_0 g_1} N^{-1/\nu} \right), \quad \lambda_- \rightarrow \lambda_c. \tag{45}$$

If N is sufficiently large, specifically, if $N \gg (g_0\gamma_1/\gamma_0 g_1)^\nu$, then Γ_E becomes independent of basis dimension at the critical point,

$$\Gamma_E(\lambda; N_1, N_2) \sim \frac{\alpha/\nu}{\frac{\alpha}{\nu} + \frac{1-\alpha}{\nu}} = \alpha. \tag{46}$$

If N_1 and N_2 are sufficiently large and the scaling postulate is applicable, then plots of $\Gamma_E(\lambda; N_1, N_2)$ versus λ for various different choices of N_1 and N_2 will intersect at λ_c and their value at that point will be the critical exponent, α. To calculate Γ_E, we will need to calculate $\partial E_N/\partial\lambda$, but that is easily done by taking advantage of the Hellmann-Feynman theorem,

$$\frac{\partial E_N}{\partial \lambda} = \left\langle \frac{\partial H(\lambda)}{\partial \lambda} \right\rangle = \langle W \rangle. \tag{47}$$

Kais et al. [10] considered various simple model quantum mechanical problems and showed that the Δ_E and Γ_E plots had an intersection point, and that the resulting estimates for the critical parameters were reasonable. They also considered the two-electron atom, using a specialized basis set, and were able to accurately reproduce

the expected results for λ_c and α. They then used the method with a simplified model Hamilton to predict critical charges for atoms throughout the periodic table [11]. They have more recently formulated the method for use with Gaussian basis sets, the basis sets used in most quantum chemistry software packages [12].

4 SUMMATION OF PERTURBATION SERIES

4.1 THE EFFECTS OF SINGULARITIES ON CONVERGENCE

Suppose that the Hamiltonian operator for a problem of interest is similar to that of a problem that can be solved more easily. Let H_0 be the Hamiltonian whose eigenfunctions and eigenvalues are known and then write the true Hamiltonian in the form

$$H = H_0 + \lambda v, \quad v = H - H_0, \tag{48}$$

where v is the *perturbation* and λ is the *perturbation parameter*, such that $\lambda = 0$ corresponds to the problem we can easily solve while $\lambda = 1$ corresponds to the physical problem. The eigenvalue $E(\lambda)$ of the Schrödinger equation

$$(H_0 + \lambda v)\Psi = E(\lambda)\Psi \tag{49}$$

can be treated as a continuous function of a variable λ in the complex plane. In contrast to the parameters considered previously in this chapter, which represented physical properties, this λ is an artificial construction that does not have to have any physical meaning. Nevertheless, the extrapolation from $E(0)$ to $E(1)$ will depend on the mathematical structure of the function $E(\lambda)$; in particular, on its singularities.

Eq. (49) is typically solved recursively. For example, if we substitute series expansions for the wavefunction and the eigenvalue,

$$\Psi \sim \sum_{k=0}^{\infty} \Psi_k \lambda^k, \quad E \sim \sum_{k=0}^{\infty} E_k \lambda^k, \tag{50}$$

and then collect terms according to power of λ, we obtain a set of equations that can be solved one after the other. At zeroth order we have only the unperturbed problem, $(H_0 - E_0)\Psi_0 = 0$, which by assumption we know how to solve. The equation obtained by collecting terms proportional to λ^1 can be solved in terms of the zeroth-order wavefunction Ψ_0, and so on to higher orders, with each subsequent equation solvable in terms of solutions from lower orders. However, for realistic problems the computational cost increases considerably with the level of recursion.

We have been using the symbol "$\sim$." Let us now define it. The power series for E is an example of an *asymptotic series*. The qualitative idea is that each additional term is a correction to the sum of the preceding terms, but it is worthwhile to describe

this more precisely.[2] Let S_n be the *partial sum* of the series at arbitrary order n,

$$S_n(\lambda) = \sum_{k=0}^{n} E_k \lambda^k. \tag{51}$$

Then the relation "$\sim$," called *asymptotic equality*, is defined as follows: Consider a function $E(\lambda)$ and an infinite power series $\sum_{k=0}^{\infty} E_k \lambda^k$. If for any value of n,

$$\lim_{\lambda \to 0} \frac{E(\lambda) - S_n}{\lambda^n} = 0, \tag{52}$$

then $E(\lambda)$ is *asymptotic* to the infinite series,

$$E \sim \sum_{k=0}^{\infty} E_k \lambda^k, \quad \lambda \to 0. \tag{53}$$

Let us write

$$E - S_n \sim \mathcal{O}(\lambda^{n+1}) \tag{54}$$

to say that the error from truncating the infinite power series at order n goes to 0 at least as fast as λ^{n+1} in the limit $\lambda \to 0$. A theorem from complex analysis tells us that the asymptotic series of a function, in terms of a given variable about a given point, is unique. There exists only one series that will satisfy Eq. (52).

Asymptotic equality is a formal way of stating what is perhaps obvious: If we use S_n as an approximation for $E(\lambda)$, the error $\mathcal{O}(\lambda^{n+1})$ in the limit $\lambda \to 0$ goes to 0 at least as fast as λ^{n+1}. The implication is that for sufficiently small λ the error in S_2 will be less than the error in S_1, the error in S_3 will be less than that in S_2, and so on. It is important to emphasize, however, that this holds only for *sufficiently small* λ. How small is "sufficient" is not always obvious. For perturbation theories, as formulated in Eq. (48), the evaluation point is $\lambda = 1$, so the partial sums can converge only if the E_k decrease with k, which is not always the case in practice. For realistic physical problems, the computational cost of obtaining the coefficients of the series coefficients can increase very significantly with increasing order. It can be quite discouraging if that newly computed term at next higher order in fact *lowers* the accuracy!

Let us study this phenomenon with some simple model problems. If we have an explicit expression for $E(\lambda)$, we can calculate the series coefficients E_n using Taylor's theorem:

$$E_k = \frac{1}{k!} \frac{d^k E}{d\lambda^k}\bigg|_{\lambda=0}. \tag{55}$$

[2]For a more detailed exposition of the theory of asymptotic series, see Baker and Graves-Morris [13].

Of course, in practical calculations we will go in the other direction—we will calculate the E_k in order to estimate $E(\lambda)$. However, Taylor's theorem is useful for obtaining asymptotic series of known functions for the purpose of method development and testing.

Our first example will be the 2×2 matrix eigenvalue problem of Eq. (4), but rather than solve this at various discrete values of λ and interpolate between them as we did for the molecular potential energy curve in Section 2, here we will treat this as a perturbation theory. The advantage of a perturbation theory is that it constructs a function of λ just from information at a single particular point where the analysis is simpler. Let us suppose that we know the eigenvalues and eigenvectors of the operators h_{11} and h_{22} in Eq. (4). We could solve for the asymptotic series for $E(\lambda)$ recursively using the standard, but laborious, methods of perturbation theory, but in this case, because we have the explicit exact solution for $E(\lambda)$ (Eq. 5), we can just use Taylor's theorem to calculate the series coefficients. Because the series is unique, the result will be the same.

We can apply quadratic approximants to an asymptotic series by parameterizing the polynomial coefficients to the series coefficients rather than to values of the function itself. Consider an arbitrary function $E(\lambda)$ with asymptotic series in the form of Eq. (53). As before, we define three polynomials,

$$P(\lambda) = p_0 + p_1\lambda + p_2\lambda^2 + \cdots + p_{M_p}\lambda^{M_p}, \tag{56}$$

$$Q(\lambda) = 1 + q_1\lambda + q_2\lambda^2 + \cdots + q_{M_q}\lambda^{M_q}, \tag{57}$$

$$R(\lambda) = r_0 + r_1\lambda + r_2\lambda^2 + \cdots + r_{M_r}\lambda^{M_r}. \tag{58}$$

If we know the series coefficients through order n, then we will have $n + 1$ simultaneous linear equations for the polynomial coefficients. This constrains the choice of polynomial degrees according to

$$M_p + M_q + M_r = n - 1, \tag{59}$$

so that we have the same number of equations as coefficients. We now construct a quadratic equation

$$Q(\lambda)E^2 - P(\lambda)E + R(\lambda) \sim \mathcal{O}(\lambda^{n+1}), \tag{60}$$

substituting for E the asymptotic series (Eq. 53). We multiply through by the polynomials, collect the terms into separate equations according to powers of λ, and ignore any terms proportional to λ raised to powers $n + 1$ or higher. This gives us $n + 1$ simultaneous linear equations for the coefficients. The approximants are then given by

$$S(\lambda) = \frac{1}{2Q(\lambda)}\left[P(\lambda) \pm \sqrt{P(\lambda)^2 - 4Q(\lambda)R(\lambda)}\right]. \tag{61}$$

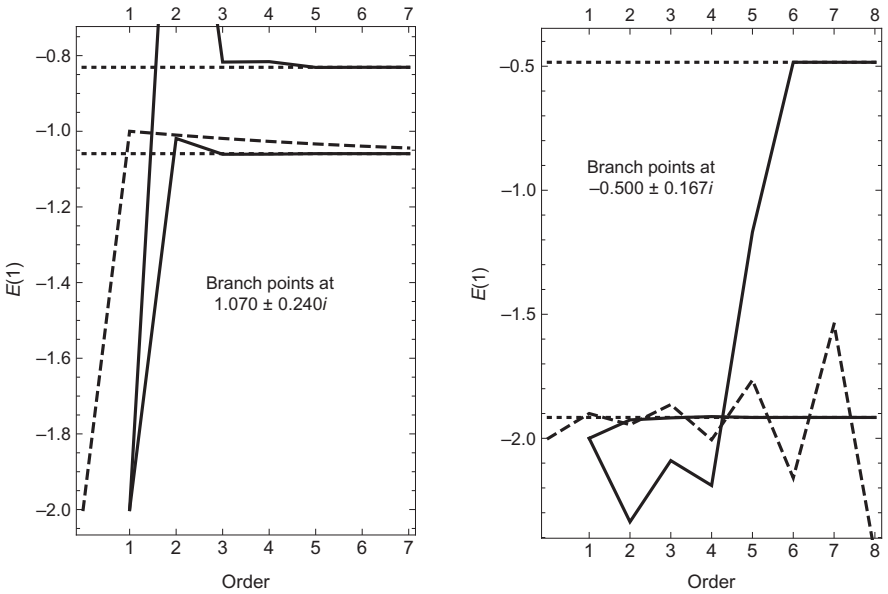

FIG. 6

Convergence of perturbation series for 2 × 2 matrix eigenvalue problems in the form of Eq. (4), summed at $\lambda = 1$. The parameters are $h_{11} = -2$, $h_{22} = -1$, $v_{11} = 1$, $v_{22} = 0.11$, $w = 0.1$ for the *left panel*, and $h_{11} = -2$, $h_{22} = -1.5$, $v_{11} = 0.1$, $v_{22} = 1.0$, $w = 0.15$ for the *right*. *Dashed line* segments are drawn between the results for the partial sums. *Solid line* segments are drawn between results for each branch of a sequence of quadratic approximants. The *dotted lines* show the exact values of the two eigenvalues.

We obtain a different approximant for each choice of the polynomial degrees, and for any $n > 1$ there will be more than one choice for given n, according to Eq. (59). Let us indicate the polynomial degrees with the symbol $[M_p/M_q, M_r]$. A common practice is to calculate approximants with increasing n in a *diagonal* sequence, with polynomial degrees increasing in concert, such as

$$[0/0,0],\ [1/0,0],\ [1/0,1],\ [1/1,1],\ [2/1,1],\ldots. \tag{62}$$

In general, the number of branch points in the $[M_p/M_q, M_r]$ approximant is

$$n_{\mathrm{bp}} = \max(2M_p, M_q + M_r). \tag{63}$$

The diagonal sequence (62) ensures that the approximant will always have an even number of branch points, which is consistent with the Katz theorem for matrix eigenvalue problems.

Fig. 6 shows how singularity structure can affect the convergence of an asymptotic series. The dashed curves show the results from the partial sums S_n evaluated

Table 1 Locations of Branch Points of the Quadratic Approximants Used for the Left Panel of Fig. 6

Order	**2**	**3**	**4**	**5**	**6**	
Index	[1/0, 0]	[1/0, 1]	[1/1, 1]	[2/1, 1]	[2/1, 2]	Exact
Branch points	$1.920 \pm 0.560i$	$1.075 \pm 0.229i$	$1.076 \pm 0.230i$ $-7.1 \pm 0.001i$	$2 \times 10^{10} \pm 8 \times 10^{7}i$	$1.070 \pm 0.240i$ -1×10^{9} 1×10^{9}	$1.070 \pm 0.240i$

at $\lambda = 1$ while the solid curves show the results for both branches from sequences of quadratic approximants. The left panel is for a case in which the partial sums converge steadily, but slowly, to the correct answer. A well-known theorem from complex analysis states that the partial sums of an asymptotic series will converge only if there are no singular points within the circular region of the complex plane centered at the expansion point ($\lambda = 0$ in this case) with radius equal to the distance to the evaluation point ($\lambda = 1$ in this case). The *circle of convergence* is the circular region centered at the expansion point with radius equal to the distance to the nearest singularity in the complex plane. For the left panel, the evaluation point is just barely inside this circle. The partial sums converge, but the convergence is slow. The lower branch of the quadratic approximant, in contrast, converges almost immediately, already giving essentially the exact result for the lower eigenvalue by third order. The upper branch of the quadratic approximant performs very poorly at first, but by third order begins a quick convergence to the upper eigenvalue.

The convergence pattern of the quadratic approximants can be explained by the convergence patterns for the branch point location. As shown in Table 1, there is a close correspondence between the two. At second order, there is no branch point in the vicinity of the correct location. As a result, the accuracy of the quadratic approximant in the left panel for the ground state at second order is no better than that of the partial sum. The series we are summing is the asymptotic expansion of the lower eigenvalue and it is only via the branch point that anything can be inferred from it about the upper eigenvalue. Therefore, it is not surprising that the second-order result for the upper eigenvalue is not accurate at all. By third order, the branch point is already being modeled accurately, and the results for both eigenvalues are quite good. The superfluous branch points, which first appear at fourth order, are placed far away from the vicinities of the expansion point and the evaluation point.

The right panel of the figure shows the convergence for a case in which the singular points are in the negative half-plane and within the circle of convergence. Because the singular points are far from the evaluation point, the first-order partial sum gives a very accurate estimate, but then it *diverges* with increasing order, as expected from the partial-sum convergence theorem. The bracketing behavior, alternating above and below the correct result, is due to the fact that the real part

Table 2 Locations of Branch Points of the Quadratic Approximants Used for the Right Panel of Fig. 6

Order	2	3	4	5	6	
Index	[1/0, 0]	[1/0, 1]	[1/1, 1]	[2/1, 1]	[2/1, 2]	Exact
Branch points	−0.589	−0.298	−0.352	$-0.502 \pm 0.170i$	$-0.500 \pm 0.167i$	$-0.5 \pm 0.167i$
	−679	−4.1	3.63	$24 \pm 2.7i$	$-3\times10^{12} \pm 7\times10^{11}i$	

of the singular points is negative. Despite the divergence of the partial sums, the sequence of quadratic approximants converges well. The lower branch is already very accurate by second order. The approximant's branch point structure, shown in Table 2, is not quite right below fifth order, with a single branch point on the real axis approximately between the two true singular points, but this has little effect on the accuracy of the lower branch because the evaluation point is far away. The upper branch of the approximant converges only when the branch point positions become very accurate, at sixth order.

Fig. 7 treats a more complicated situation. The function is

$$E(\lambda) = -[(\lambda_1 - \lambda)(\lambda_1^* - \lambda)]^{1/2} - [(\lambda_2 - \lambda)(\lambda_2^* - \lambda)]^{1/2},$$
$$\lambda_1 = 0.65 + 0.2i, \quad \lambda_2 = 1.3 + 0.2i. \tag{64}$$

The behavior of the partial sums of the asymptotic series is determined by the singular points at λ_1 and λ_1^*, which determine the circle of convergence. Because the evaluation point $\lambda = 1$ is outside that circle, the partial sums must diverge. However, in contrast to the previous case, in which the singularities were in the negative half-plane and the partial sums initially converged to the correct result before diverging, these singularities are in the positive half-plane, between the expansion point and the evaluation point. As shown in the figure, the partial sums in this situation are useless even at low order. The basic problem is that the partial summation approximant, $S_n(\lambda)$ of Eq. (51), is a polynomial. A polynomial can have no singularity at any finite point in the complex plane. It can accurately approximate singular functions in nonsingular regions, but not in regions affected by singularities. In this case, $S_n(\lambda)$ is attempting to extrapolate through a pair of branch points and fails.

This function has four branches, corresponding to the different possible choices for the signs of the two square roots. The quadratic approximant, by construction, has only two branches. Fig. 7 shows that it convergences to the two branches of the function connected by the branch points at λ_1 and λ_1^*. Again, the accuracy of the approximant corresponds to the accuracy of the branch point positions, listed in Table 3. Note in the figure the glitch in the convergence of the lower branch at fifth order. The lower-order approximants have only two branch points, and therefore focus their efforts on accurately describing the dominant singularities at λ_1 and λ_1^*.

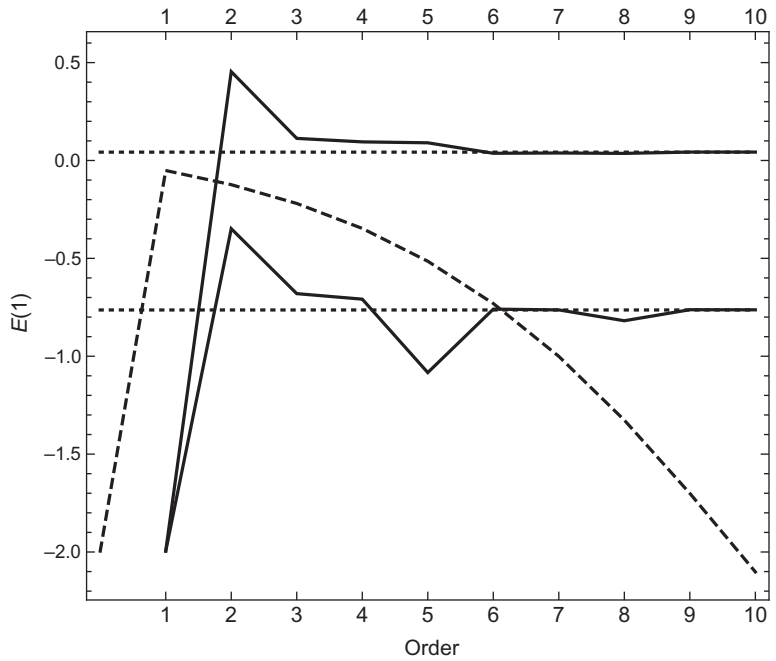

FIG. 7

Convergence of perturbation series summed at $\lambda = 1$ for the function $E(\lambda)$ of Eq. (64), which has two pairs of branch points in the positive half-plane. *Dashed line* segments are drawn between the results for the partial sums. *Solid line* segments are drawn between results for each branch of a sequence of quadratic approximants. The *dotted lines* show the exact values of the two eigenvalues connected by the innermost of the branch-point pairs.

The $[2/1, 1]$ approximant is the first in the sequence to have four branch points, because the discriminant $P^2 - 4QR$ is now a polynomial of fourth degree. The initial attempt in an approximant sequence to model a singularity is typically relatively inaccurate. $S_{[2/1,1]}$ in this case gives a poor description of the singularities at λ_2 and λ_2^* and a slightly less accurate description of the dominant singularities. This is remedied at sixth order. Beyond seventh order the results do not significantly improve, because after that, newly introduced singularities are superfluous. The true function has only four singularities.

The quadratic approximant is a special case of a more general construction called an *algebraic approximant*. Let us generalize Eq. (60) to arbitrary degree m,

$$P_{M_m}(\lambda)E^m + P_{M_{m-1}}(\lambda)E^{m-1} + P_{M_{m-2}}(\lambda)E^{m-2} + \cdots + P_{M_0}(\lambda) \sim \mathcal{O}(\lambda^{n+1}), \qquad (65)$$

where P_{M_j} is a polynomial of degree M_j. Of the $\sum_j (M_j + 1)$ coefficients, one is always arbitrary. (Dividing both sides of the equation by one of the coefficients will have no effect on the equations that determine the coefficients.) Usually, one sets

Table 3 Locations of Branch Points of the Quadratic Approximants of Fig. 7

Order	**2**	**3**	**4**	**5**	
Index	[1/0, 0]	[1/0, 1]	[1/1, 1]	[2/1, 1]	
Branch points	$0.948 \pm 0.393i$	$0.676 \pm 0.230i$	$0.660 \pm 0.218i$	$0.680 \pm 0.187i$ $1.811 \pm 0.115i$	
Order	**6**	**7**	**8**	**9**	
Index	[2/1, 2]	[2/2, 2]	[3/2, 2]	[3/2, 3]	Exact
Branch points	$0.649 \pm 0.200i$ $1.293 \pm 0.024i$	$0.650 \pm 0.200i$ $1.300 \pm 0.026i$	$0.650 \pm 0.201i$ $1.291 \pm 0.053i$ -3.282 -3.286	$0.650 \pm 0.200i$ $1.297 \pm 0.086i$ $1.303 \pm 0.116i$	$0.65 \pm 0.2i$ $1.3 \pm 0.2i$

the zeroth-order coefficient of the polynomial multiplying E^m to 1. Substituting the asymptotic series for E and collecting terms according to power of λ yields, as before, a set of simultaneous linear equations that determine the values of the polynomial coefficients. The approximant is obtained as the numerical solution of

$$P_{M_m}(\lambda)S^m + P_{M_{m-1}}(\lambda)S^{m-1} + P_{M_{m-2}}(\lambda)S^{m-2} + \cdots + P_{M_0}(\lambda) = 0, \tag{66}$$

with λ set to the evaluation point. For high-order series, it is wise to use a recursive algorithm in order to control numerical instabilities from round-off error [14,15].

An algebraic approximant of degree m has m branches. This is appealing, because the functions that describe realistic physical problems often have many more than two branches. However, the rate of convergence of the approximants is highest for the principal branch (i.e., the branch for which the asymptotic series was calculated) and slows significantly for higher branches, especially for branches that interact only weakly with the principal branch. High-degree approximants can be useful if the series coefficients are known to high order. However, in practice, quadratic approximants are often adequate, especially if one is only interested in studying the principal branch of the function. They provide a simple explicit analytical expression for $S(\lambda)$. Furthermore, they are able to model the effects on the principal eigenvalue of many different branches with appropriately placed branch points. Of course, all the branch points of a quadratic approximant connect with a single second branch, rather than to different branches as in higher-degree algebraic approximants and in the true solution. The higher branch of the quadratic approximant will have to simultaneously model multiple branches, modeling different branches in different regions of λ.

4.2 SUMMATION METHODS FOR VARIOUS PROBLEMS

4.2.1 Molecular vibrations

Consider the vibrational spectrum of a diatomic molecule. For a first approximation, it is usually treated as a harmonic oscillator, with Hamiltonian

$$H_0 = -\frac{\hbar^2}{2\mu}\frac{d^2}{d\xi^2} + \frac{1}{2}k\xi^2, \tag{67}$$

where μ is the reduced mass of the molecule and the coordinate $\xi = x - x_e$ is the deviation from the equilibrium bond distance. This Hamiltonian gives one of the few exactly solvable Schrödinger equations. Its eigenfunctions are well known and are commonly used as a basis set for more complicated problems.

Of course, actual molecular potential curves are not symmetric in ξ (see Fig. 2). However, the harmonic oscillator is a reasonable approximation for low-lying eigenstates of tightly bound molecules, for which only the immediate vicinity of the bottom of the potential well has a significant probability distribution. For a more accurate description, a common practice is to add a polynomial perturbation, the simplest being a cubic term,

$$H = H_0 + \lambda\xi^3. \tag{68}$$

This slightly broadens the well in the direction of stretched bond lengths and makes it steeper for compressed bond lengths, which is physically reasonable. The eigenvalues and eigenfunctions of H can be calculated from a matrix eigenvalue problem in the harmonic oscillator basis. We can expect square-root branch points in the complex λ-plane, according to the Katz theorem.

Fig. 8 compares the qualitative shapes of the unperturbed and perturbed potential energy curves. Suppose that a wavefunction is initially localized in the well of the potential. There will be a nonzero probability of its tunneling out of the well, giving dissociated free atoms. There must be a critical point, corresponding to the largest λ at which the molecule is stable. The critical point in this case is at $\lambda = 0$, because for any nonzero λ the potential will eventually drop to negative infinity on one side of the well. This is just an artifact of the form chosen for the potential. However, it causes the radius of the circle of convergence for the perturbation theory in λ to be zero. There is a singularity at the origin of the complex λ-plane.

The functional form of this singularity is complicated—certainly more complicated than the branch points of an algebraic approximant. Nevertheless, algebraic approximants give convergent results for the perturbation theory in λ [15]. They manage to accomplish this using clusters of algebraic branch points near the origin.

For practical applications to molecular vibrations, the singularity at the origin is not usually a problem, because adequate accuracy can be obtained from moderately low orders off the perturbation theory. For vibrations of polyatomic molecules, square-root branch points of the real axis tend to be the more serious problem. Eigenstates that are degenerate in the zeroth-order approximation can be affected differently by the perturbation and have their degeneracy broken. This can result in

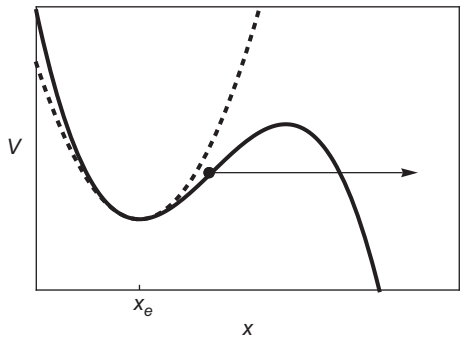

FIG. 8

Illustration of the instability of the cubic oscillator potential energy (*solid curve*) to tunneling, as opposed to the harmonic oscillator potential (*dotted curve*), which is stable.

branch points close to the origin that can seriously degrade the convergence of partial sums. Algebraic approximants have been applied with success to perturbation series for excited vibrational states of molecules with three or four atoms [16]. Fourth-degree approximants seem best for states with moderately high excitation, with no further improvement from going to higher degree. For very high excitation levels, there is a proliferation of branch points that in practice overwhelms the approximants' ability to distinguish between the effects of interactions with so many different states. In such cases, repartitioning the Hamiltonian, redefining H_0 so as to selectively shift the levels of the unperturbed eigenstates and thereby change the positions of branch points, can help [17].

4.2.2 Dimensional perturbation theory

As another example of a theory in which singularity analysis plays an important role, consider the electronic Schrödinger equation treated with dimensional perturbation theory, which, in effect, formulates the electronic structure calculation as a vibrational problem. The Schrödinger equation is generalized to a space of arbitrary dimension D and then expressed in appropriately scaled units such that D appears only as an effective mass multiplying the derivatives in the kinetic energy operator. In the limit $D \to \infty$ the electrons adopt a fixed configuration at the minimum of an effective potential energy surface. Within first-order perturbation theory in terms of $\delta = 1/D$, the electrons vibrate harmonically. Higher orders bring in anharmonic corrections.

One can prove that the ground-state energy of the Schrödinger equation in the dimension-scaled units has a second-order pole at $\delta = 1$, and writing the energy as an interpolation between the first-order series in δ at the $\delta \to 0$ limit and the pole at the $D \to 1$ limit results in a surprisingly reasonable estimate for the physical energy at $D = 3$ [18]. However, the attempt to systematically improve the accuracy simply by adding in higher powers of δ fails because the partial sums of the series

diverge. This is another perturbation theory with a zero radius of convergence, with a complicated singular point at the origin of the complex δ-plane.

Convergent summation approximants for the δ series have been developed [19]. However, the high-order series coefficients are difficult to calculate, and in practice, the effect of the singularity at the origin on the behavior of the low-order coefficients is small. Furthermore, it results from generic behavior of the kinetic energy operator, not from the detailed form of the potential energy. This means that the large-order behavior of the δ series from an approximate model such as the Hartree-Fock approximation that simplifies the potential energy but not the kinetic energy should be similar to that of the exact series. Herschbach et al. [20] have taken advantage of this to construct a very simple yet quite accurate expression for the ground-state energy of the two-electron isoelectronic sequence (H^-, He, Li^+, etc.) as a function of atomic number Z. What they did is interpolate the correlation energy (the difference between the exact energy and the energy from the Hartree-Fock approximation) between the first-order δ series and the $\delta = 1$ pole, evaluate this at $D = 3$, and then add it to the accurately known Hartree-Fock energy. The effect of the singularity at the origin mostly canceled out.

4.2.3 Møller-Plesset perturbation theory

The classic perturbation theory for calculations of electronic structure is the Møller-Plesset (MP) perturbation theory (also called many-body perturbation theory). The Hamiltonian is partitioned so that the zeroth-order part H_0 is the sum of one-electron Fock operators. A perturbation parameter z is introduced into the full Hamiltonian according to

$$H(z) = H_0 + z(H_{\text{phys}} - H_0), \tag{69}$$

where H_{phys} is the actual physical Hamiltonian. Evaluation of the perturbation series at $z = 1$ yields an approximate solution of the physical problem. The zeroth-order approximation is qualitatively similar to the exact solution, and as a result, the eigenvalue $E(z)$ does not have a singularity at the origin. However, the zeroth-order Hamiltonian omits from the potential energy the terms that explicitly describe interelectron repulsion, replacing those terms with a one-electron mean field.

The Hartree-Fock approximation is solved within a basis-set expansion for the wavefunction. Hence, the perturbation theory yields a series in z that is asymptotic to the ground-state eigenvalue of the matrix representation of $H(z)$ in that basis set. This is an asymptotic series for the FCI solution as a function of the perturbation parameter. Let us call this solution $E_N(z)$, where N is the size of the basis set. Thus, the MP series gives an approximate solution for $E_N(z)$, which in turn is an approximate solution for $E(z)$, the exact ground-state eigenvalue of $H(z)$.

The first-order series in z gives the Hartree-Fock approximation for the energy. The second-order series (MP2) is quite popular, on account of its balance of computational efficiency and reasonable accuracy for predicting molecular geometries, but for quantitative calculations of energy differences, higher-order series are needed. MP3, MP4, and MP5 are available in standard quantum chemistry software packages. MP4,

in particular, has long been of interest as the highest-order MP method for which the computational cost is not unreasonable.

Traditionally, the MP series was evaluated as a partial sum, simply adding up the terms of the series. This is now known to be inadequate [21] because it does not take into account the singularity structure of the energy as a function of z. The singularity structure of the exact MP energy function $E(z)$ is quite interesting [22]. To begin with, there are the expected Katz-type branch points. These are square-root branch points at discrete complex-conjugate points in the complex z plane, which connect pairs of eigenstates. Then there are critical points, of two different kinds.

The perturbation operator $z(H_{\text{phys}} - H_0)$ contains the term $z \sum_{j,k} r_{jk}^{-1}$, the potential energy for interelectron repulsion in H_{phys}, and the term $-zV_0$, where V_0 is the mean field repulsive potential for a given electron obtained by averaging over the exact potential with the Hartree-Fock orbitals. The interelectron term for increasing z on the positive real axis becomes increasingly repulsive. This is counteracted by the mean field term. V_0 itself is repulsive but the minus sign makes it an attractive potential in the perturbation operator for positive real z. If the repulsive term dominates, then the net effect of the perturbation operator will be destabilizing and there will be some value z_c beyond which the system will ionize. This will give a critical point on the positive real axis. Such singularities have been identified [22] but do not seem to be of significant importance in practice. For physically stable systems, this z_c will be quite distant from $z = 1$, while for less stable systems, a square-root branch point pair from an avoided crossing with an excited state can be expected that has smaller real part than z_c and a stronger effect on series convergence.

Consider, however, what can happen for *negative* real z. The interelectron repulsion is now multiplied by a negative number. This means that the electron-electron interaction is not repulsive, but attractive! Of course, this is completely nonphysical, but we know from complex analysis that singularities in nonphysical regions of the z-plane can affect the behavior of $E(z)$ in the physical region. The term $-zV_0$ is now a repulsive mean field, becoming increasingly destabilizing at increasingly negative real z. There will inevitably be a z_c beyond which the system will ionize, arranging itself into a bound cluster of mutually attractive electrons dissociated from the nuclei. This curious phenomenon was apparently first predicted in the context of nuclear physics [23], where a similar perturbation theory is used to calculate nuclear binding energies. This singularity in practice quite often has a significant effect on the MP series convergence.

Given enough terms in the z series, quadratic approximants can deal with all these singularities and give convergent summation. Although the functional form of a critical point in $E(z)$ is much more complicated than a square-root branch point, the series we are summing in fact corresponds to $E_N(z)$, which has only square-root branch points. In the neighborhood of z_c, $E_N(z)$ uses a clustering of branch points in complex-conjugates pairs close to the real axis to mimic the true singularity structure there.

The situation with MP4, however, is more complicated. The quadratic approximant at fourth order has only two branch points. If $E_N(z)$ has significant singularity structure in both the positive and negative half-planes, the approximant will have

a tendency to place its branch points somewhere in between, thereby introducing singular behavior in a nonsingular region and failing to model any of the true singularities. An easy way to mitigate this effect is to use the quadratic approximant in combination with a bilinear conformal mapping of the complex plane [24]. Let us replace z with a new variable u according to

$$u = \frac{z}{1 - \lambda + \lambda z}, \quad z = \frac{(1 - \lambda)u}{1 - \lambda u}, \tag{70}$$

where λ is an arbitrary free parameter. The expression for z can be expanded in a Taylor series in u and then substituted into the perturbation series. If the coefficients of the series in z are E_k, then the coefficients of the new u series are

$$\tilde{E}_k(\lambda) = \sum_{j=1}^{k} \binom{k-1}{j-1} \lambda^{k-j} (1 - \lambda)^j E_j, \quad \binom{n}{m} = \frac{n!}{(n-m)!\,m!}. \tag{71}$$

This mapping has two fixed points, at $z = 0$ and $z = 1$, where z and u have the same value. Thus, the mapping leaves the zeroth-order solution and the physical solution unchanged. All other points in the complex plane are shifted, depending on the value chosen for λ. This is illustrated in Fig. 9, which shows the locations in the complex u-plane of singularities for the hydrogen fluoride molecule as a function of λ.

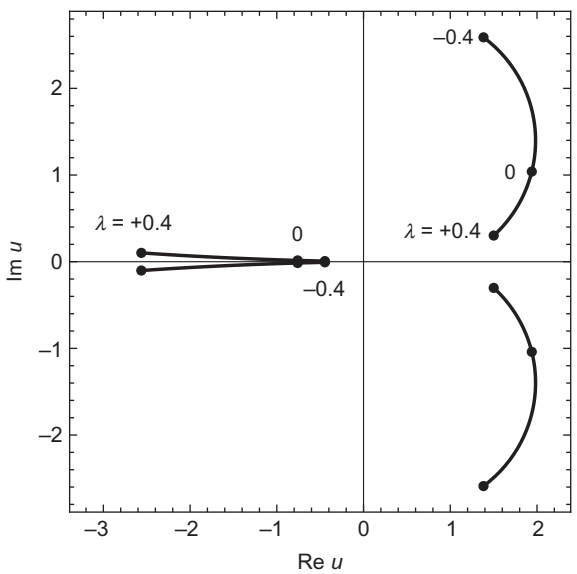

FIG. 9

Shift in singularity positions from a bilinear conformal mapping of the complex plane. The values of the parameter λ, of Eqs. (70), are indicated. The original singularity positions ($\lambda = 0$) correspond to the hydrogen fluoride molecule with the aug-cc-pVDZ basis.

A negative value of λ shifts the branch points in the positive half-plane away from the origin, and the critical point (modeled in $E_N(z)$ by a pair of square-root branch points very close to the real axis) is shifted toward the origin. The reverse happens with a positive value of λ. This usually makes it possible to force the MP4 approximant to accurately model singularity structure in one half-plane while ignoring that in the other half-plane. The MP4qλ method [21,25] is a reasonably systematic procedure for implementing this idea.

Because of the convergence problems with the partial sums, MP4 has been mostly supplanted in practice by the CCSD(T) method, a hybrid of coupled-cluster theory and perturbation theory that has only a slightly higher computational cost but is somewhat more reliable. The MP4qλ results seem to be comparable in accuracy to CCSD(T) for atoms and for molecules near their equilibrium geometries. Both methods fail as bonds become significantly stretched. MP4qλ fails somewhat sooner than CCSD(T), but at least has the advantage of a built-in diagnostic, in the position of its branch points. If the conformal mapping cannot significantly shift the branch points, this indicates that the branch points are too close to the fixed points, and in practice it means that the accuracy of the approximant will suffer.

REFERENCES

[1] Goodson DZ. Mathematical methods for physical and analytical chemistry. Hoboken, NJ: Wiley; 2011 [Chapters 6 and 7; For brief and relatively painless introduction to this subject].
[2] Arfken GA. Mathematical methods for physicists. Orlando, FL: Academic Press; 1985.
[3] Katz A. The analytic structure of many-body perturbation theory. Nucl Phys 1962;29:353.
[4] Goodson DZ. On the use of quadratic approximants to model diatomic potential energy curves. Mol Phys 2012;110:1681.
[5] Jordan KD. Applications of analytic continuation in the construction of potential energy curves. Int J Quant Chem Symp Ser 1975;9:325.
[6] Olsen J, Jørgensen P, Koch H, Balkova A, Bartlett RJ. Full configuration-interaction and state of the art correlation calculations on water in a valence double-zeta basis with polarization functions. J Chem Phys 1996;104:8007.
[7] Baker JD, Freund DE, Hill RN, Morgan JD, III. Radius of convergence and analytic behavior of the $1/Z$ expansion. Phys Rev A 1990;41:1247.
[8] Privman V. Radius of convergence and analytic behavior of the $1/Z$ expansion. Finite size scaling and numerical simulations of statistical systems. Singapore: World Scientific; 1990.
[9] Fisher ME, Barber MN. Scaling theory for finite-size effects in the critical region. Phys Rev Lett 1972;28:1516.
[10] Neirotto JP, Serra P, Kais S. Electronic structure critical parameters from finite-size scaling. Phys Rev Lett 1997;79:3142.
[11] Sergeev AV, Kais S. Critical nuclear charges for N-electron atoms. Int J Quant Chem 1999;75:533.

[12] Moy W, Kais S, Serra P. Finite size scaling with gaussian basis sets. Mol Phys 2008;106:203.
[13] Baker GAJ, Graves-Morris P. Padé approximants. Cambridge: Cambridge University Press; 1996.
[14] Sergeev AV. A recursive algorithm for Padé-Hermite approximations. USSR Comput Math Math Phys 1986;26:17.
[15] Sergeev AV, Goodson DZ. Summation of asymptotic expansions of multiple-valued functions using algebraic approximants: Application to anharmonic oscillators. J Phys A Math Gen 1998;31:4301.
[16] Duchko AN, Bykov AD. Resummation of divergent perturbation series: Application to the vibrational states of formaldehyde molecule. J Chem Phys 2015;143:154102.
[17] Surjan PR, Szabados A. Optimized partitioning in perturbation theory: Comparison to related approaches. J Chem Phys 2000;112:4438.
[18] Doren DJ, Herschbach DR. Accurate semiclassical electronic structure from dimensional singularities. Chem Phys Lett 1985;118:115. Loeser JG. Atomic energies from the large-dimension limit. J Chem Phys 1986;86:5635. Frantz DD, Herschbach DR. Lewis electronic structures as the large-dimension limit for H_2^+ and H_2 molecules. Chem Phys 1988;126:59.
[19] Elout MO, Goodson DZ, Elliston CD, Huang SW, Sergeev AV, Watson DK. Improving the convergence and estimating the accuracy of summation approximants of $1/D$ expansions for Coulombic systems. J Math Phys 1998;39:5112.
[20] Herschbach DR, Loeser JG, Virgo WL. Exploring unorthodox dimensions for two-electron atoms. J Phys Chem A 2017;121:6336.
[21] Goodson DZ. Resummation methods. WIREs Comput Mol Sci 2012;2:743.
[22] Sergeev AV, Goodson DZ, Wheeler SE, Allen WD. On the nature of the Møller-Plesset critical point. J Chem Phys 2005;123:064105.
[23] Baker GA, Jr. Singularity structure of the perturbation series for the ground-state energy of a many-fermion system. Rev Mod Phys 1971;43:479.
[24] Feenberg E. Invariance property of the Brillouin-Wigner perturbation series. Phys Rev 1956;103:1116.
[25] Goodson DZ. A summation procedure that improves the accuracy of the fourth-order Møller-Plesset perturbation theory. J Chem Phys 2000;113:6461.